

# Effects of Ligand Substitutions on the Rotation Rate of Indenyl Ligands in Bis(2-aryindenyl)zirconocenes by NMR Line-Shape Analysis and Relaxation in the Rotating Frame

Gregg M. Wilmes,<sup>†</sup> Marcia B. France,<sup>‡</sup> Stephen R. Lynch,<sup>†</sup> and Robert M. Waymouth<sup>\*,†</sup>

Departments of Chemistry, Stanford University, Stanford, California 94305, and Washington and Lee University, Lexington, Virginia 24450

Received September 10, 2003

Unbridged bis(2-aryindenyl)metallocene complexes, such as bis(2-phenylindenyl)zirconium dichloride (**1a**), when treated with appropriate activators are active catalyst precursors for the production of elastomeric polypropylene. The proposed mechanism for polymerization involves isomerization of the catalyst between geometries of differing stereoselectivity on a time scale slower than polymer chain growth. As the rotation of the 2-aryindenyl ligand is proposed to result in the different catalyst geometries, the rate at which this rotation occurs is of interest for the interpretation of the behavior of these complexes. A series of zirconocenes {bis(2-phenylindenyl)zirconium dimethyl (**1b**), bis(2-phenylindenyl)zirconium dibenzyl (**1c**), bis(2-(3,5-di-*tert*-butylphenyl)indenyl)zirconium dimethyl (**2b**), and bis(2-(3,5-di-*tert*-butylphenyl)indenyl)zirconium dibenzyl (**2c**)}, varying both in the indenyl ligand framework and the  $\sigma$ -ligand, has been synthesized. The rotation rates of the methyl-substituted metallocenes are too fast to be determined by standard NMR techniques such as EXSY, line-shape analysis, or magnetization transfer experiments. On-resonance spin–lattice relaxation in the rotating frame ( $T_{1\rho}$ ) has been used to determine the rate of rotation of the aryl ligands in **1b**, **1c**, and **2b** and allowed comparison with the rates obtained for the benzylated species by line-shape analysis. The nature of both the  $\pi$  and the  $\sigma$  ligand systems affects the rate, with sterically bulky substituents resulting in slower rotation. The effect of the  $\sigma$  ligand is substantially stronger than that of the  $\pi$  ligand.

## Introduction

Soluble homogeneous metallocene-based catalysts for the stereospecific polymerization of propylene have provided new insights into the mechanism of olefin polymerization and provided a toolbox for the generation of new polyolefins.<sup>1,2</sup> The physical properties of a polypropylene are dependent on its stereochemical microstructure—the relative configurations of the methyl substituents along the polymer chain. This microstructure, in turn, is dependent on the nature of the catalyst. Metallocene-based catalysts have been studied in great depth, and a number of simple rules correlating their structure and the symmetry of their ligand frameworks to the polypropylene they produce have been developed and exploited to produce a variety of materials ranging from tacky gums to tough, rigid plastics.<sup>1</sup>

One form of this polymer that is of particular interest is thermoplastic elastomeric polypropylene.<sup>3–37</sup> This

material was first described by Natta as a soluble extract of a polymer made with a heterogeneous catalyst system and was postulated to consist of isotactic blocks capable of cocrystallization across polymer chains and atactic blocks that provide flexibility.<sup>3–6</sup> It was discovered in our laboratories that fluxional unbridged bis(2-aryindenyl)zirconocenes such as bis(2-phenylindenyl)zirconium dichloride (**1a**), when activated with an appropriate cocatalyst, form active catalyst systems for the production of elastomeric polypropylene.<sup>14,15,17–40</sup>

(5) Natta, G. *J. Polym. Sci.* **1959**, *34*, 531–549.

(6) Natta, G.; Crespi, G. U.S. Patent 3,175,999, 1965.

(7) Collette, J. W.; Tullock, C. W.; MacDonald, R. N.; Buck, W. H.; Su, A. C. L.; Harrel, J. R.; Mulhaupt, R.; Anderson, B. C. *Macromolecules* **1989**, *22*, 3851–3858.

(8) Mallin, D. T.; Rausch, M. D.; Lin, Y. G.; Dong, S.; Chien, J. C. W. *J. Am. Chem. Soc.* **1990**, *112*, 2030–2031.

(9) Chien, J. C. W.; Llinas, G. H.; Rausch, M. D.; Lin, G. Y.; Winter, H. H.; Atwood, J. L.; Bott, S. G. *J. Am. Chem. Soc.* **1991**, *113*, 8569–8570.

(10) Gauthier, W. J.; Collins, S. *Macromolecules* **1995**, *28*, 3779–3786.

(11) Nele, M.; Mohammed, M.; Xin, S.; Collins, S.; Dias, M. L.; Pinto, J. C. *Macromolecules* **2001**, *34*, 3830–3841.

(12) Kukral, J.; Lehmus, P.; Feifel, T.; Troll, C.; Rieger, B. *Organometallics* **2000**, *19*, 3767–3775.

(13) Dietrich, U.; Hackmann, M.; Rieger, B.; Klinga, M.; Leskelae, M. *J. Am. Chem. Soc.* **1999**, *121*, 4348–4355.

(14) Dreier, T.; Erker, G.; Frohlich, R.; Wibbeling, B. *Organometallics* **2000**, *19*, 4095–4103.

(15) Dreier, T.; Bergander, K.; Wegelius, E.; Frohlich, R.; Erker, G. *Organometallics* **2001**, *20*, 5067–5075.

<sup>†</sup> Stanford University.

<sup>‡</sup> Washington and Lee University.

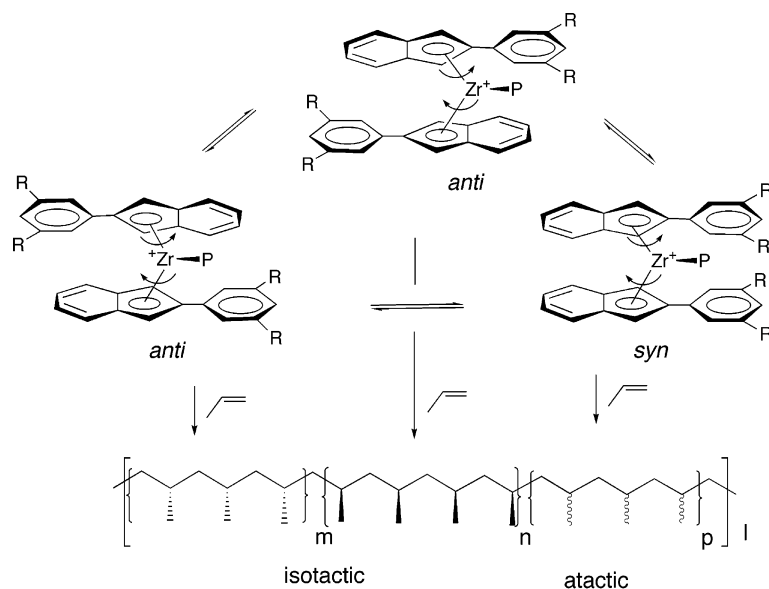
(1) Resconi, L.; Cavallo, L.; Fait, A.; Piemontesi, F. *Chem. Rev.* **2000**, *100*, 1253–1345.

(2) *Metallocene-Based Polyolefins: Preparation, Properties, and Technology*; Scheirs, J., Kaminsky, W., Eds.; Wiley: New York, 2000.

(3) Natta, G.; Mazzanti, G.; Crespi, G.; Moraglio, G. *Chim. Ind. (Milan)* **1957**, *39*, 275–283.

(4) Natta, G. *Atti Accad. Naz. Lincei* **1958**, *24*, 246–253; *Chem. Abstr.*, 1958, **52**, 19413h.

## Scheme 1. Proposed Mechanism for the Formation of Elastomeric Polypropylene



The  $^{13}\text{C}$  NMR spectra of the polypropylenes produced were consistent with an atactic/isotactic stereoblock polymer.<sup>18,23,34,41</sup> The crystal structure of **1a** showed two low-energy conformations: a  $C_2$ -symmetric anti conformer reminiscent of bridged catalysts for the isotactic polymerization of propylene and a  $C_s$ -symmetric syn conformer of the proper geometry for producing atactic polypropylene. It was thus hypothesized that the active catalytic species was undergoing a conformational exchange between stereoselective and nonstereoselective forms at a rate slower than polymer chain growth to enable the formation of isotactic and atactic blocks (Scheme 1). Recent studies have questioned the role of

the achiral syn conformers as the source of atactic stereosequences;<sup>15,38–40</sup> nevertheless, the role of the conformational dynamics on the stereoselectivity of these metallocenes is strongly indicated by the influence of monomer concentration on the type and frequency of stereoregions.<sup>18,23,30–32</sup>

The competition between the conformational dynamics of the metallocene and monomer insertion leads to a very high sensitivity of these catalyst systems to modifications of the ligand structure,<sup>19,21,22,25,26,28,29</sup> metal,<sup>20</sup> or cocatalyst,<sup>33</sup> or of the reaction conditions, such as monomer concentration, temperature, additives, or solvent.<sup>27,30,33</sup> Studies of all of these tunable features have shown that these fluxional metallocene catalyst systems are quite versatile but exceedingly complex as the relative rates of interconversion, propagation, and chain termination are likely to be sensitive to any modification of the catalyst or polymerization conditions.<sup>31,34,38–40</sup>

As the rotation of the 2-arylindenyl ligands is a key factor determining the nature of the polypropylene produced, it is clearly of interest to measure the rate of this process.<sup>15,17,20,42</sup> The rotation rates of **1a** and its more sterically hindered analogue bis(2-(3,5-di-*tert*-butylphenyl)indenyl)zirconium dichloride (**2a**) have eluded measurement as they are too rapid to be determined by standard techniques such as EXSY,<sup>43</sup> line-shape analysis,<sup>44</sup> or magnetization transfer.<sup>45</sup> Com-

(16) Miller, S. A.; Bercaw, J. E. *Organometallics* **2002**, *21*, 934–945.

(17) Schneider, N.; Schaper, F.; Schmidt, K.; Kirsten, R.; Geyer, A.; Brintzinger, H. H. *Organometallics* **2000**, *19*, 3597–3604.

(18) Coates, G. W.; Waymouth, R. M. *Science* **1995**, *267*, 217–219.

(19) Hauptman, E.; Waymouth, R. M.; Ziller, J. W. *J. Am. Chem. Soc.* **1995**, *117*, 11586–11587.

(20) Bruce, M. D.; Coates, G. W.; Hauptman, E.; Waymouth, R. M.; Ziller, J. W. *J. Am. Chem. Soc.* **1997**, *119*, 11174–11182.

(21) Petoff, J. L. M.; Bruce, M. D.; Waymouth, R. M.; Masood, A.; Lal, T. K.; Quan, R. W.; Behrend, S. J. *Organometallics* **1997**, *16*, 5909–5916.

(22) Kravchenko, R.; Masood, A.; Waymouth, R. M. *Organometallics* **1997**, *16*, 3635–3639.

(23) Bruce, M. D.; Waymouth, R. M. *Macromolecules* **1998**, *31*, 2707–2715.

(24) Petoff, J. L. M.; Agoston, T.; Lal, T. K.; Waymouth, R. M. *J. Am. Chem. Soc.* **1998**, *120*, 11316–11322.

(25) Kravchenko, R.; Masood, A.; Waymouth, R. M.; Myers, C. L. *J. Am. Chem. Soc.* **1998**, *120*, 2039–2046.

(26) Lin, S.; Hauptman, E.; Lal, T. K.; Waymouth, R. M.; Quan, R. W.; Ernst, A. B. *J. Mol. Catal. A: Chem.* **1998**, *136*, 23–33.

(27) Petoff, J. L. M.; Myers, C. L.; Waymouth, R. M. *Macromolecules* **1999**, *32*, 7984–7989.

(28) Witte, P.; Lal, T. K.; Waymouth, R. M. *Organometallics* **1999**, *18*, 4147–4155.

(29) Tagge, C. D.; Kravchenko, R. L.; Lal, T. K.; Waymouth, R. M. *Organometallics* **1999**, *18*, 380–388.

(30) Lin, S.; Tagge, C. D.; Waymouth, R. M.; Nele, M.; Collins, S.; Pinto, J. C. *J. Am. Chem. Soc.* **2000**, *122*, 11275–11285.

(31) Nele, M.; Collins, S.; Dias, M. L.; Pinto, J. C.; Lin, S.; Waymouth, R. M. *Macromolecules* **2000**, *33*, 7249–7260.

(32) Wilmes, G. M.; Lin, S.; Waymouth, R. M. *Macromolecules* **2002**, *35*, 5382–5387.

(33) Wilmes, G. M.; Polse, J. L.; Waymouth, R. M. *Macromolecules* **2002**, *35*, 6766–6772.

(34) Lin, S.; Waymouth, R. M. *Acc. Chem. Res.* **2002**, *35*, 765–773.

(35) Dankova, M.; Kravchenko, R. L.; Cole, A. P.; Waymouth, R. M. *Macromolecules* **2002**, *35*, 2882–2891.

(36) Waymouth, R. M.; Hauptman, E.; Coates, G. W. *PCT Int. Appl. WO* 9525757, 1995.

(37) Waymouth, R. M.; Hauptman, E.; Coates, G. W. U.S. Patent 5,969,070, 1999.

(38) Busico, V.; Cipullo, R.; Kretschmer, W.; Talarico, G.; Vacatello, M.; Castelli, V. V. *Macromol. Symp.* **2002**, *189*, 127–141.

(39) Busico, V.; Cipullo, R.; Kretschmer, W. P.; Talarico, G.; Vacatello, M.; Castelli, V. V. *Angew. Chem., Int. Ed.* **2002**, *41*, 505–508.

(40) Busico, V.; Castelli, V. V. A.; Aprea, P.; Cipullo, R.; Segre, A.; Talarico, G.; Vacatello, M. *J. Am. Chem. Soc.* **2003**, *125*, 5451–5460.

(41) Busico, V.; Cipullo, R.; Segre, A. L.; Talarico, G.; Vacatello, M.; Castelli, V. V. A. *Macromolecules* **2001**, *34*, 8412–8415.

(42) Knickmeier, M.; Erker, G.; Fox, T. *J. Am. Chem. Soc.* **1996**, *118*, 9623–9630.

(43) Perrin, C. L.; Dwyer, T. J. *Chem. Rev.* **1990**, *90*, 935–967.

pounds in which the two chloro  $\sigma$  ligands were replaced with methyl groups were prepared (**1b** and **2b**), but these complexes also exhibit very fast rates of ligand rotation. In contrast, measurements of the rate of exchange of the more sterically hindered benzyl analogue, bis(2-phenylindenyl)zirconium dibenzyl (**1c**), have been successful,<sup>17,20</sup> but did not allow comparisons among metallocenes with different  $\sigma$  substituents.<sup>15</sup> We now report the use of on-resonance spin–lattice relaxation in the rotating frame ( $T_{1\rho}$ )<sup>46–51</sup> to determine the rate of rotation of the aryl ligands in **1b**, **2b**, and **1c**, thus allowing the first quantitative comparisons among these compounds. The  $T_{1\rho}$  methodology has been used predominantly in measurements of protein dynamics,<sup>52</sup> and has rarely been applied to organometallic systems;<sup>53</sup> nevertheless it offers a valuable means of determining rates of molecular dynamics on a microsecond time scale.

## Results

The metallocenes bis(2-phenylindenyl)zirconium dichloride (**1a**), dimethyl (**1b**), and dibenzyl (**1c**) were prepared according to literature procedures.<sup>20,36,37</sup> Bis(2-(3,5-di-*tert*-butylphenyl)indenyl)zirconium dichloride (**2a**) and dimethyl (**2b**) were prepared as previously described.<sup>32</sup> Bis(2-(3,5-di-*tert*-butylphenyl)indenyl)zirconium dibenzyl (**2c**) was synthesized by treatment of **2a** with benzylmagnesium chloride in tetrahydrofuran.

The <sup>1</sup>H NMR spectra of all dimethyl and dichloro compounds exhibited a single cyclopentadienyl (Cp) resonance down to 150 K, indicative of time-averaged symmetry, consistent with rapid indenyl rotation. In CDCl<sub>2</sub>F, the Cp peak of compound **1b** starts to show significant line broadening around 170 K and becomes a relatively flat broad resonance in the baseline (approximately the coalescence point) at 150 K. Such behavior indicates a very rapid rotation of the indenyl ligands at room temperature; however, it was not possible to achieve a temperature at which the rate of rotation is slow enough to show two sets of signals for the Cp protons, thus precluding the use of line-shape analysis, magnetization transfer, or EXSY to measure the rate. The dichloro compound **1a** does not show appreciable line broadening even at 150 K in CDCl<sub>2</sub>F.

The rapid conformational dynamics of **1a**, **1b**, **2a**, and **2b** prompted us to investigate other methods of quantifying the rate of rotation of the indenyl ligands. Attempts at using temperature-dependent NOESY methods<sup>17,43</sup> failed due to poor resolution of the aromatic signals of complexes **1a** and **1b** at low temperatures in

suitable solvents. Measurements of longitudinal relaxation in the rotating frame,  $T_{1\rho}$ , on coalesced lines can be used to measure rates on the microsecond time scale.  $T_{1\rho}$  is measured by spin-locking the magnetization in the *XY*-plane by application of a magnetic field ( $H_1$ ) perpendicular to the steady magnetic field ( $H_0$ ). Since the magnetization of the sample and  $H_1$  fields are parallel, no torque is exerted on the net magnetization. Seen in the rotating frame, the spin-locking field is stationary and the relaxation along the *Y*-axis is longitudinal and is characterized by the time constant  $T_{1\rho}$ .<sup>54</sup> Chemical exchange in the range of  $k = 10^2$ – $10^6$  s<sup>-1</sup> can generate contributions to  $T_{1\rho}$  although they do not affect the longitudinal relaxation,  $T_1$ .<sup>46,48</sup> Provided that other processes, such as scalar relaxation from quadrupolar nuclei, do not contribute to  $T_{1\rho}$ , a measurement of  $T_{1\rho}$  as a function of spin-locking field strength yields the rate constant for chemical exchange and the chemical shift difference in the region of slow exchange. Measurements of  $T_{1\rho}(\text{obs})$ , the observed time constant of longitudinal relaxation in the rotating frame, together with  $T_1$  (obtained by standard inversion–recovery techniques) can be used to calculate the component of that time constant due to exchange,  $T_{1\rho}(\text{ex})$ , according to eq 1.

$$\frac{1}{T_{1\rho}(\text{ex})} = \frac{1}{T_{1\rho}(\text{obs})} - \frac{1}{T_1} \quad (1)$$

Equation 2 describes the relationship between spin-locking field strength and  $T_{1\rho}(\text{ex})$  for an equally populated two-site model,<sup>46,47,49</sup> where  $\omega_1$  is the power of the spin-locking field (in rad·s<sup>-1</sup>),  $\Delta\nu$  is the chemical shift difference (in Hz) between the exchanging protons in the absence of chemical exchange, and  $\tau_{\text{ex}}$  is the effective lifetime of exchange.

$$T_{1\rho}(\text{ex}) = \frac{1 + \omega_1^2 \tau_{\text{ex}}^2}{(\pi \Delta\nu)^2 \tau_{\text{ex}}} \quad (2)$$

Thus, a plot of  $T_{1\rho}(\text{ex})$  versus  $\omega_1^2$  gives a line with slope =  $\tau_{\text{ex}}/(\pi \Delta\nu)^2$  and intercept =  $1/(\pi \Delta\nu)^2 \tau_{\text{ex}}$ . Rearranging these expressions gives eqs 3 and 4

$$\tau_{\text{ex}} = \left( \frac{\text{slope}}{\text{intercept}} \right)^{1/2} \quad (3)$$

$$\Delta\nu = \left( \frac{\tau_{\text{ex}}}{\pi^2 \text{slope}} \right)^{1/2} \quad (4)$$

The methodology and our experimental setup were calibrated by studies on Me<sub>2</sub>NCOCl; the results showed excellent agreement with those reported in the literature.<sup>55</sup> The  $T_{1\rho}$  method was then used to measure first-order rate constants of exchange and chemical shift differences of the Cp proton resonances of **1b** (in CDCl<sub>2</sub>F), **1c** (in *d*<sub>8</sub>-toluene), and **2b** (in CDCl<sub>2</sub>F). The Gibbs free energy of activation ( $\Delta G^\ddagger$ ) was calculated from the Eyring equation (eq 5), using the first-order rate constant,  $k = 1/\tau_{\text{ex}}$ ,<sup>56–58</sup> Planck's constant,  $h$ ;

(54) Traficante, D. D. In *Encyclopedia of NMR*; Grant, D. M., Harris, R. K., Eds.; Wiley: New York, 1996; Vol. 6, pp 3398–4003.

(55) Braun, S.; Kalinowski, H.-O.; Berger, S. *150 and More Basic NMR Experiments: A Practical Course*, 2nd ed.; VCH: Weinheim, Germany, 1998.

(44) Sandström, J. *Dynamic NMR Spectroscopy*; Academic Press: London, UK, 1982.

(45) Hoffman, R. A.; Forsén, S. *Prog. NMR Spectrosc.* **1966**, *1966*, 15–204.

(46) Deverell, C.; Morgan, R. E.; Strange, J. H. *Mol. Phys.* **1970**, *18*, 553–559.

(47) Stilbs, P.; Moseley, M. E. *J. Magn. Reson.* **1978**, *31*, 55–61.

(48) Lambert, J. B.; Nienhuis, R. J.; Keepers, J. W. *Angew. Chem., Int. Ed. Engl.* **1981**, *20*, 487–500.

(49) Wang, Y.-S. *Magn. Reson. Chem.* **1989**, *27*, 1134–1141.

(50) Wang, Y.-S. *Concepts Magn. Reson.* **1992**, *4*, 327–337.

(51) Wang, Y.-S. *Concepts Magn. Reson.* **1993**, *5*, 1–18.

(52) Blackledge, M. J.; Brüschweiler, R.; Griesinger, C.; Schmidt, J. M.; Xu, P.; Ernst, R. R. *Biochemistry* **1993**, *32*, 10960–10974.

(53) Chopra, S.; McClung, R. E. D.; Jordan, R. B. *J. Magn. Reson.* **1984**, *59*, 361–372.



**Table 1. Chemical Shift Differences, Rotation Rate Constants, and Free Energy of Activation from  $T_{1\rho}$  for Compounds **1b**, **2b**, and **1c****

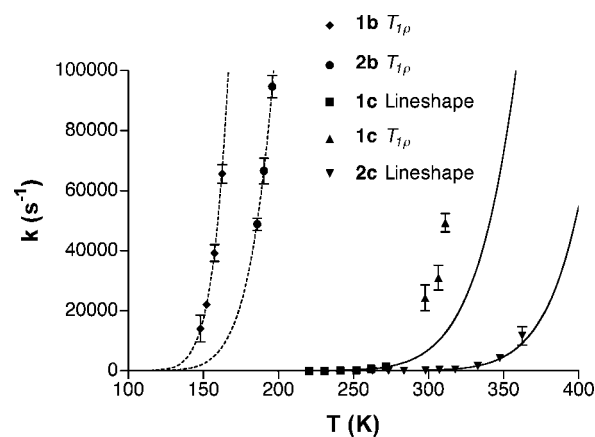
compd	$T$ (K)	$\Delta\nu$ (ppm)	$k$ ( $s^{-1}$ )	$\Delta G^\ddagger$ (kcal/mol)
<b>1b</b>	148 ± 0.5	2.14 ± 0.54	14 000 ± 4 500	5.65 ± 0.11
	152	1.96 ± 0.10	22 100 ± 1 200	5.68 ± 0.04
	157	1.92 ± 0.16	39 300 ± 2 700	5.71 ± 0.04
<b>2b</b>	162	1.82 ± 0.12	65 600 ± 3 100	5.73 ± 0.03
	186	1.92 ± 0.08	48 900 ± 2 000	6.71 ± 0.03
	190	1.83 ± 0.13	66 600 ± 4 300	6.76 ± 0.04
<b>1c</b>	196	1.73 ± 0.08	94 700 ± 3 700	6.84 ± 0.03
	298	1.38 ± 0.23	24 400 ± 4 300	11.45 ± 0.12
	307	1.38 ± 0.18	31 100 ± 4 100	11.66 ± 0.10
	311	1.37 ± 0.10	49 300 ± 3 100	11.56 ± 0.06

Boltzmann's constant,  $k_B$ ; temperature,  $T$ ; and ideal gas constant,  $R$ .

$$k = \frac{k_B T}{h} e^{-\Delta G^\ddagger/RT} \quad (5)$$

The temperature range over which the analyses could be performed had a lower limit near the coalescence temperature of each compound and an upper limit determined by the rate of exchange and the maximum spin-locking field strength,  $\omega_1$ , which could be generated by the instrument. At higher temperatures, no dependence of  $\omega_1$  on  $T_{1\rho}(\text{ex})$  was observed as the value of  $\omega_1^2 \tau_{\text{ex}}$  approached zero. These effects limited the applicable temperature range for the three compounds to only 10–15 K. Results are shown in Table 1. Although the compounds could not be directly compared at the same temperature, the temperatures at which they undergo exchange at similar rates can be compared. For example, the rate constant of exchange is  $39\,300 \pm 2\,700\text{ s}^{-1}$  at 157 K for compound **1b**,  $48\,900 \pm 2\,000\text{ s}^{-1}$  at 186 K for **2b**, and  $49\,300 \pm 3\,100\text{ s}^{-1}$  at 311 K for **1c**. It is clear that the addition of steric bulk to either the 3,5-positions of the 2-aryl ring or the  $\sigma$  ligand of the metal leads to a lower rate of ligand rotation.

To further check the accuracy of the  $T_{1\rho}$  method and to observe the effects of addition of steric bulk on the rate of interconversion, VT-NMR line-shape techniques<sup>44</sup> were used to measure the rotation rates of the dibenzyl compounds **1c** and **2c**. In the slow exchange regime, the spectra of these compounds are consistent with  $C_2$  symmetry: two singlets resulting from the Cp protons are observed, and the diastereotopic benzyl protons give a pair of doublets. At higher temperatures, both the Cp and benzyl resonances coalesce into singlets. Previous experiments have demonstrated that for this class of compound the exchange rate measured from the Cp resonances is the same as that measured from the benzyl resonances.<sup>17,20</sup> This observed exchange is

**Figure 1.** Exchange rates measured by line shape and  $T_{1\rho}$ .

taken to result from interconversion between the two enantiomers of the anti species. The spectrum of **1c** was examined from 221 to 272 K in  $d_8$ -toluene, that of **2c** from 263 to 362 K in  $d_2$ -1,1,2,2-tetrachlorethane. Rate constants of the exchange were obtained with the gNMR 4.1 software package.<sup>59</sup> Results are shown in Table 2.<sup>60</sup> As with the dimethyl species, the compound with the more sterically hindered ligand system had a much lower rate of exchange. For example, at ~260 K, the rate constant of exchange of **1c** was  $740\text{ s}^{-1}$  compared to  $7\text{ s}^{-1}$  for **2c**. The free enthalpy and free energy of activation for **1c** and **2c** were calculated according to the linearized Eyring equation with the substitution  $\Delta G^\ddagger = \Delta H^\ddagger - T\Delta S^\ddagger$  (Table 3). The temperature ranges over which the  $T_{1\rho}$  measurements could be made were too small to extract meaningful activation parameters. The rate constants for all four compounds measured by both techniques are shown in Figure 1 with solid lines showing the predicted rates for compounds **1c** and **2c** from the Eyring analysis from the line-shape data and dashed lines showing the best fit curve for compounds **1b** and **2b**.

## Discussion

**$T_{1\rho}$  Measurements.** The rate of interconversion for bis(2-phenylindenyl)zirconium dibenzyl (**1c**) was measured by both the  $T_{1\rho}$  method and the more standard line-shape analysis. The activation parameters from the line-shape analysis can be used to calculate the expected rate constants at a given temperature. At 298 K, for example, the rate constant for **1c** extrapolated from the activation parameters from line-shape analysis is  $6\,320 \pm 7\,250\text{ s}^{-1}$ . The value measured by  $T_{1\rho}$ ,  $24\,400 \pm 4\,300\text{ s}^{-1}$ , is approximately four times greater than the value

**Table 2. Rotation Rate Constants and Gibbs Free Energy of Activation from Line-Shape Analysis for Compounds **1c** and **2c****

<b>1c</b>			<b>2c</b>		
$T$ (K)	$k$ ( $s^{-1}$ )	$\Delta G^\ddagger$ (kcal/mol)	$T$ (K)	$k$ ( $s^{-1}$ )	$\Delta G^\ddagger$ (kcal/mol)
221 ± 0.5	22 ± 1	11.43 ± 0.04	263 ± 0.5	7 ± 1	14.32 ± 0.08
231	56 ± 3	11.55 ± 0.03	273	22 ± 2	14.28 ± 0.05
241	140 ± 7	11.65 ± 0.03	284	48 ± 3	14.39 ± 0.03
252	250 ± 250	11.90 ± 0.27	298	150 ± 9	14.48 ± 0.04
262	740 ± 245	11.10 ± 0.17	307	315 ± 17	14.50 ± 0.03
272	1590 ± 740	11.87 ± 0.25	318	530 ± 135	14.68 ± 0.16
			333	1 630 ± 400	14.66 ± 0.16
			347	4 170 ± 1 300	14.69 ± 0.21
			362	11 700 ± 3 000	14.61 ± 0.19

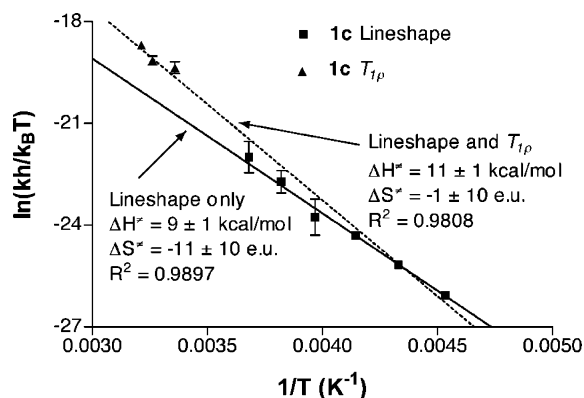


**Figure 2.** Linearized Eyring plot for ligand rotation rate of bis(2-phenylindenyl)zirconium dibenzyl.

**Table 3. Activation Parameters Obtained from Line-Shape Rate Analyses**

compd	$\Delta H^\ddagger$ (kcal/mol)	$\Delta S^\ddagger$ (eu)
<b>1c</b>	$9 \pm 1$	$-11 \pm 10$
<b>2c</b>	$13 \pm 1$	$-5 \pm 10$

predicted from the line-shape analysis. However, if an Eyring plot of the line shape and  $T_{1\rho}$  measurements is made (Figure 2), it can be seen that the linear least-squares fit of the line-shape data alone is only slightly better than that using both sets of data ( $R^2 = 0.9897$  vs  $R^2 = 0.9808$ ). Furthermore the change in calculated activation parameters between the two sets of data is on the order of the experimental error in their measurements ( $\Delta H^\ddagger = 9 \pm 1$  kcal/mol,  $\Delta S^\ddagger = -11 \pm 10$  eu for the line-shape data alone vs  $\Delta H^\ddagger = 11 \pm 1$  kcal/mol,  $\Delta S^\ddagger = -1 \pm 10$  eu for the  $T_{1\rho}$  and line-shape data together). This agreement of the  $T_{1\rho}$  technique with the more widely used line-shape analysis, though not perfect, is sufficient to provide useful comparisons between measurements made by the two methods.

Along with the rate of exchange, the  $T_{1\rho}$  technique also gives information concerning the chemical shift difference of exchanging resonances—information that cannot otherwise be obtained if temperatures well below the coalescence point are not accessible. For compound **1c**, the observed chemical shift difference of the Cp resonances at 217 K was 1.53 ppm, which compares quite well with the values obtained from the  $T_{1\rho}$  measurement ( $1.38 \pm 0.23$  ppm at 291 K).

**Effect of Ligands on Rotation Rate.** In both the dimethyl and the dibenzyl complexes, the rate of rotation was significantly slower for the 3,5-di-*tert*-butyl-substituted aryl indenyl ligands than for the 2-phenylindenyl ligand. For dibenzyl compounds **1c** and **2c**, for which the rates were measured over a temperature

range of at least 50 K, this difference in rate is reflected in the activation parameters:  $\Delta\Delta H^\ddagger = 4$  kcal/mol,  $\Delta\Delta S^\ddagger = 6$  cal/(mol·K), and at  $\sim 273$  K,  $\Delta\Delta G^\ddagger = 2.4$  kcal/mol, implying that substitution of the 2-aryindenyl ligands with sterically demanding *tert*-butyl substituents causes a significant increase in the energy barrier for ligand rotation. This comparison of activation parameters cannot be made for compounds **1b** and **2b** as these measurements were made over a very small temperature range (10–15 K). Nevertheless, as can be seen in Table 1 and Figure 1, the rate of exchange in the metallocene with the bulky substituents is again much lower than that of the 2-phenylindene complex **1b**.

The change from a methyl group to a benzyl group (**1b** vs **1c** or **2b** vs **2c**) resulted in a lower rotation rate for both indenyl ligand frameworks. The influence of the  $\sigma$ -bonded ligand is dramatic. For example, the rate constant of rotation of the dimethyl compound **1b** was  $22\,100 \pm 1\,200$  s $^{-1}$  at 152 K, whereas that of the dibenzyl **1c** at 252 K was only  $250 \pm 135$  s $^{-1}$ ; at a temperature 100 K greater, the dibenzyl compound had a rate of exchange almost 100 times lower than the dimethyl.

**Effect of Rotation Rate on Propylene Polymerization.** For the mechanism presented in Scheme 1 to be valid, the turnover frequency for polymer chain growth at a metal center must be greater than the rate of ligand conformational exchange. Measurements of the rate of propylene polymerization by **1a**/MAO in toluene solution have been made by monitoring propylene consumption. Over a range of monomer concentrations from 1.16 to 3.81 M and a range of zirconium concentrations from 0.5 to 2  $\mu$ M, a second-order rate constant,  $k_p$  for the rate expression shown in eq 6, could be calculated from the maximum rate of polymerization of each run to be  $\sim 45$  M $^{-1}$  s $^{-1}$  at 293 K, assuming all of the zirconium was catalytically active.<sup>30</sup> In neat propylene ([propylene]  $\approx 11$  M) the turnover frequency at each metal site ( $k_p[\text{monomer}]$ ) would be  $\sim 500$  s $^{-1}$ .

$$\frac{-\partial[\text{monomer}]}{\partial t} = k_p[\text{Zr}^*][\text{monomer}] \quad (6)$$

Measurements of the rate of 1-hexene polymerization by [*rac*-(C<sub>2</sub>H<sub>4</sub>(1-indenyl)<sub>2</sub>ZrMe)]/[MeB(C<sub>6</sub>F<sub>5</sub>)<sub>3</sub>] by stopped-flow and isotopic labeling techniques gave  $k_p = 6.3 \pm 0.6$  M $^{-1}$  s $^{-1}$  at 293 K,<sup>61,62</sup> which would give a turnover frequency of  $\sim 50$  s $^{-1}$  in neat 1-hexene. The above estimates for the rates of monomer insertion are slower than the rates of rotation measured for the dibenzyl compound **1c** ( $24\,400$  s $^{-1}$  at 298 K) (and estimated to be several orders of magnitude slower than **1b** and **2b**) and similar to that measured for the sterically hindered **2c** ( $150$  s $^{-1}$  at 298 K). As previously discussed,<sup>17,20</sup> the dimethyl and dibenzyl complexes are likely to be imperfect models of the active catalyst species, which is a zirconium cation with one  $\sigma$  ligand that can vary from a hydride to a polymer chain with a molecular weight of hundreds of thousands of grams per mole. Moreover, it is clear that the nature of the cocatalyst and the attendant counteranion should have an impor-

(56) In the  $T_{1\rho}$  literature, the relationship between rate constant and mean lifetime for equally populated species is typically expressed as  $k = 1/2\tau_{\text{ex}}$ , where  $k$  is the unidirectional rate constant. We have chosen to present  $k$  as the overall rate constant  $k = 1/\tau_{\text{ex}}$ , which is typically reported in line-shape studies. This distinction is more thoroughly explained in refs 57 and 58.

(57) Faller, J. W. *Adv. Organomet. Chem.* **1977**, *116*, 211–239.

(58) Green, M. L. H.; Wong, L.-L. *Organometallics* **1992**, *11*, 2660–2668.

(59) Budzelaar, P. H. M. *gNMR*, version 4.1; Adept Scientific: Herts, 1999 (www.adeptscience.com).

(60) The exchange rates for compound **1c** differ somewhat from those reported in ref 20. Different solvents were used for the two measurements, and in toluene, the chemical shift of the benzyl protons varied considerably with temperature.

(61) Liu, Z. X.; Somsook, E.; Landis, C. R. *J. Am. Chem. Soc.* **2001**, *123*, 2915–2916.

(62) Liu, Z. X.; Somsook, E.; White, C. B.; Rosaaen, K. A.; Landis, C. R. *J. Am. Chem. Soc.* **2001**, *123*, 11193–11207.

tant influence on the conformational dynamics.<sup>33,63</sup> As the relatively small increase in the steric bulk of the  $\sigma$  ligand from methyl to benzyl significantly slows the rotation rate, it seems reasonable that increasing the bulk further—to a polymer chain—could slow the rotation rate down sufficiently such that it is competitive with monomer insertion. Thus, the measured rates are consistent with competitive monomer insertion and isomerization as shown in Scheme 1 for the *tert*-butyl-substituted metallocenes, but for the less sterically hindered 2-phenylindenyl systems, the mechanism of Scheme 1 is only consistent with the observed behavior if the rate of ligand rotation for the cationic active species is slower than that measured for the neutral complexes.

Previous propylene polymerization studies<sup>32</sup> using catalyst precursors **1–2** showed a large difference in the polymers produced. The isotactic pentad fraction, as measured by <sup>13</sup>C NMR, increased from 44% with **1a** activated by methylaluminoxane (MAO) in bulk monomer to 78% with **2a** under the same conditions. According to the mechanism shown in Scheme 1, this increase in isotacticity could be attributed to a number of factors: an increase in the population of the anti conformers relative to the syn conformers,<sup>32,39,64</sup> an increase in the propagation rates of the anti forms relative to the syn, or a slower rate of conversion among the accessible conformations of the catalyst species. The differences in rotation rates of compounds **1b** vs **2b** and **1c** vs **2c** provide a partial explanation for the differences in polymerization behavior for the two catalyst systems, as a slower rate of ligand rotation (as has been observed with the 2-(3,5-di-*tert*-butylphenyl)indenyl ligand) would lead to longer isotactic blocks and therefore a higher observed degree of isotacticity.<sup>23</sup>

The <sup>13</sup>C NMR spectra of polypropylenes synthesized with the sterically hindered metallocene **2a**<sup>32</sup> and bis(2-(3,5-di-*tert*-butyl-4-methoxyphenyl)indenyl)zirconium dichloride<sup>28,38–40</sup> are consistent with a mechanism in which the catalyst isomerizes between two enantiomeric anti conformations, with little if any contribution from the achiral syn isomer (Scheme 1,  $p = 0$ ). Thus, the higher tacticity observed for the sterically hindered metallocene is a consequence both of a slow rate of conformational dynamics and the predominance of stereoselective anti conformations in solution.<sup>32</sup>

The lower stereoselectivity of the less sterically hindered metallocene **1a** relative to the *tert*-butyl-substituted catalysts may be due either to a contribution from the achiral syn isomer, as previously proposed (Scheme 1),<sup>34</sup> or to a situation in which the rate of catalyst isomerization is on the same order as the rate of propylene insertion.<sup>20,31</sup> In the latter case, as some population of catalyst sites might have rates of isomerization faster than monomer insertion, this would lead to atactic sequences. The results of the present study are consistent with both interpretations, as these studies clearly indicate that the rate of ligand rotation for the 2-phenylindenyl catalyst is faster than that of the *tert*-butyl-substituted catalysts. The role of the syn isomer in generating atactic stereosequences from met-

allocenes **1a** remains, in our opinion, an open question. While low-temperature NMR experiments have provided no unambiguous evidence to date for the syn isomers,<sup>15,17,20</sup> both model studies<sup>24,35</sup> and theoretical calculations<sup>17,64,65</sup> indicate that it is a competent conformation to enchain the monomer. Busico has recently proposed<sup>39,40</sup> that for both the unsubstituted and substituted 2-arylindenyl catalysts the syn isomer is not an intermediate in these polymerizations, but the experimental evidence to date provides no clear reason to rule out either mechanism.

## Conclusions

The rates of ligand rotation of catalyst precursors for the polymerization of stereoblock elastomeric polypropylene, bis(2-phenylindenyl)zirconium dimethyl, and bis(2-(3,5-di-*tert*-butylphenyl)indenyl)zirconium dimethyl were measured for the first time by NMR measurements of spin–lattice relaxation in the rotating frame ( $T_{1\rho}$ ). These results were compared to rate measurements of bis(2-phenylindenyl)zirconium dibenzyl and bis(2-(3,5-di-*tert*-butylphenyl)indenyl)zirconium dibenzyl using variable-temperature NMR line-shape analysis. The addition of steric bulk to either the  $\pi$  or the  $\sigma$  ligand framework significantly reduced the rate of ligand rotation, with the  $\sigma$  ligand having the greater effect. Although the rate of ligand rotation for the dimethyl compounds is much greater than any reasonable estimate of propylene insertion (which would not allow the formation of stereoblock polypropylene as in Scheme 1), the strong effect of the nature of the  $\sigma$  ligand on rotation rate suggests that the growing polymer chain, and possibly the nature of the cocatalysts, may be important factors in modulating the dynamic behavior of these catalyst systems.

## Experimental Section

**General Comments.** All manipulations were carried out under an inert nitrogen atmosphere with standard Schlenk or drybox techniques.  $\text{CDCl}_2\text{F}$  was prepared by the literature procedure<sup>66</sup> and dried over molecular sieves prior to use. *d*<sub>8</sub>-Toluene was dried over sodium/benzophenone; 1,1,2,2-*d*<sub>2</sub>-tetrachloroethane was dried over calcium hydride prior to use. All metallocenes were synthesized according to previously published procedures.<sup>18,20,32,36,37</sup>

**Synthesis of (2-(3,5-*t*-Bu<sub>2</sub>Ph)Ind)<sub>2</sub>ZrBn<sub>2</sub> (2c).** (2-(3,5-*t*-Bu<sub>2</sub>Ph)Ind)<sub>2</sub>ZrCl<sub>2</sub> (0.445 g, 0.579 mmol) was dissolved in 60 mL of tetrahydrofuran and the solution was cooled to  $-78^\circ\text{C}$ . Benzylmagnesium chloride (1.0 M in ethyl ether, 2.3 mL, 2.3 mmol) was added via syringe. The reaction mixture was stirred under N<sub>2</sub> for 30 min, warmed to room temperature, and stirred at room temperature overnight. The tetrahydrofuran was removed in vacuo and replaced with toluene. The toluene solution was filtered and concentrated. The toluene was layered with pentane and placed in a  $-40^\circ\text{C}$  freezer. The mother liquor was removed, and the remaining orange microcrystalline powder was dried in vacuo to give 0.078 g of product (15%). <sup>1</sup>H NMR ( $\text{C}_6\text{D}_6$ , 300 MHz, 365 K):  $\delta$  7.66 (d, 4 H,  $J = 1.8$  Hz, Ph-2,6), 7.59 (t, 2 H,  $J = 1.8$  Hz, Ph-4), 7.22 (m, 4 H, CH<sub>2</sub>Ph-3,5), 7.19 (m, 4 H, CH<sub>2</sub>Ph-2,6), 6.94 (m, 2 H, CH<sub>2</sub>Ph-4), 6.87 (m, 4 H, Ind-5,6), 6.69 (br s, 4 H, Ind-4,7), 6.32 (br s, 4 H, Cp), 1.49 (s, 36 H, *t*-Bu), 0.74 (br s, 4 H, CH<sub>2</sub>).

(63) Further studies are underway to probe the influence of various cocatalysts on the conformational dynamics of these systems.

(64) Maiti, A.; Sierka, M.; Andzelm, J.; Golab, J.; Sauer, J. *J. Phys. Chem. A* **2000**, *104*, 10932–10938.

(65) Pietsch, M. A.; Rappe, A. K. *J. Am. Chem. Soc.* **1996**, *118*, 10908–10909.

(66) Siegel, J. S.; Anet, F. A. L. *J. Org. Chem.* **1988**, *53*, 2629–2630.

**NMR Measurements.** NMR experiments were recorded on a Varian Unity Inova 300- or 500-MHz spectrometer with a 5-mm broadband switchable probe. NMR spectra were acquired and processed with VNMR 6.1C software.  $^1\text{H}$  chemical shifts were referenced relative to tetramethylsilane by internal residual solvent protons.

$T_{1\rho}$  values were measured as a function of spin-lock power and temperature by varying the spin-lock time. The pulse sequence for measuring  $T_{1\rho}$  was  $90^\circ\text{-X-(spin-lock)}\text{-Y-Acquire}$ . A continuous wave spin-lock was used. The phase of the pulse, spin-lock, and receiver were incremented  $90^\circ$  with each scan, with a delay of 5 times  $T_1$  between scans. The spin-lock power was determined by measuring a  $90^\circ$  pulse at varying transmitter power and converting the pulse width into field strength (in rad/s). The frequency of the spectrum was centered 5–20 Hz away from the Cp peak so that the intensity could be measured accurately without off-resonance effects due to imperfect receiver balancing. The determination of rates by  $T_{1\rho}$  is an on-resonance technique, but is valid as long as the difference

between the resonance frequency and the pulse frequency ( $20\text{ Hz} = 125\text{ rad/s}$ ) is much lower than the spin-locking field strength ( $9\,800\text{--}140\,000\text{ rad/s}$ ).

**Acknowledgment.** We thank the BP Chemical Company and the National Science Foundation for financial support. G.M.W. is the grateful recipient of a William R. and Sarah Hart Kimball Stanford Graduate Fellowship. M.B.F. thanks the NSF for an ROA grant and Washington and Lee University for a Hewlett–Mellon grant. Helpful discussions and technical support from Mahesh Mahanthappa, Prof. John Brauman, and Dr. Lois Durham are gratefully acknowledged.

**Supporting Information Available:** Experimental details for NMR analysis, representative plots, and error analysis. This material is available free of charge via the Internet at <http://pubs.acs.org>.

OM034166V